Evaluation of clinical IMRT treatment planning using the gATE Monte Carlo simulation platform for absolute and relative dose calculations

Saadia Benhalouche, Dimitris Visvikis, Amandine Le Maitre, Olivier Pradier, Nicolas Boussion

Evaluation of clinical IMRT treatment planning using the GATE Monte Carlo simulation platform for absolute and relative dose calculations

S. Benhalouche[a)]
INSERM UMR 1101 LaTIM, CHRU Morvan, 29609 Brest, France

D. Visvikis
INSERM UMR 1101 LaTIM, CHRU Morvan, 29609 Brest, France and Department of Radiotherapy, CHRU Morvan, 29609 Brest, France

A. Le Maitre
INSERM UMR 1101 LaTIM, CHRU Morvan, 29609 Brest, France

O. Pradier and N. Boussion
INSERM UMR 1101 LaTIM, CHRU Morvan, 29609 Brest, France and Department of Radiotherapy, CHRU Morvan, 29609 Brest, France

Purpose: The objective of this study was to evaluate and validate the use of the Geant4 application for emission tomography (GATE) Monte Carlo simulation platform for clinical intensity modulated radiotherapy (IMRT) dosimetry studies.
Methods: The first step consisted of modeling a 6 MV photon beam linear accelerator (LINAC), with its corresponding validation carried out using percent depth dose evaluation, transverse profiles, tissue phantom ratio, and output factor on water phantom. The IMRT evaluation was performed by com-paring simulation and measurements in terms of absolute and relative doses using IMRT dedicated quality assurance phantoms considering seven different patient datasets.
Results: Concerning the LINAC simulated model validation tissue phantom ratios at 20 and 10 cm in water TPR^{20}_{10} obtained from GATE and measurements were 0.672 ± 0.063 and 0.675, respec-tively. In terms of percent depth dose and transverse profiles, error ranges were, respectively: $1.472\% \pm 0.285\%$ and $4.827\% \pm 1.323\%$ for field size of 4×4, 5×5, 10×10, 15×15, 20×20, 25×25, 30×30, and 40×40 cm^2. Most errors were observed at the edge of radiation fields because of higher dose gradient in these areas. Output factors showed good agreement between simulation and measurements with a maximum error of 1.22%. Finally, for IMRT simulations considering seven pa-tient datasets, GATE provided good results with a relative error of $0.43\% \pm 0.25\%$ on absolute dose between simulated and measured beams (measurements at the isocenter, volume 0.125 cm^3). Planar dose comparisons were also performed using gamma-index analysis. For the whole set of beams con-sidered the mean gamma-index value was 0.497 ± 0.152 and $90.8\% \pm 3.6\%$ of the evaluated dose points satisfied the 5% / 4 mm criterion.
Conclusions: These results show that GATE allows reliable simulation of complex beams in radio-therapy after an accurate LINAC modeling is validated. A simple cross-calibration procedure pro-posed in this work allows obtaining absolute dose values even in complex fields.

Key words: Monte Carlo simulation, GATE, dosimetry, dose calculation, IMRT treatment plan

I. INTRODUCTION

The validation of dosimetric accuracy within the context of advanced techniques for radiotherapy treatment, including intensity modulated radiotherapy (IMRT), volumetric modulated arc therapy (VMAT) or RapidArc® (Varian Medical Systems, Palo Alto, CA), as well as in the use of dedicated devices such as CyberKnife and/or TomoTherapy (Accuray®, Sunnyvale, CA) is necessary to ensure reliable patient treatment delivery. This is one of the reasons behind the use of different Monte Carlo (MC) codes allowing the modeling of linear accelerators, having shown through different studies being able to accurately calculate clinical radiotherapy dose distributions.[1–4] Other Monte Carlo codes were used for the simulation of different linear accelerator (LINAC) models, like PENELOPE for the simulation of Varian Clinacs.[5] The BEAMnrc/DOSXYZnrc code including full accelerator head modeling was also used to simulate complex treatments with Elekta Linacs and Tomotherapy systems.[6] In this particular approach, a specific methodology using position probabilities was proposed in order to take dynamic movements into account. In the clinical point of view, commercially available treatment planning systems (TPS) like MONACO (Elekta) begin to include MC-based dose calculation,[7] even if full MC-modeling and full MC-computation remain out of reach due to the required calculation time.

Based on the Geant4 Monte Carlo toolkit, Geant4 application for emission tomography (GATE) is a collaborative development aiming to provide an open source platform able to perform complex simulations based on simple microcommands. This user friendly MC simulation environment has facilitated the widespread use of this platform within the field of imaging tomography.[8,9]

On the other hand, GATE has been also used in a number of other domains like brachytherapy[10] and microcomputed tomography where doses were calculated using voxelized realistic phantoms.[11] In order to further enhance the applicability and hence utilization of the GATE platform, for dosimetry applications,[12–14] a new version [GATE v6.0 w (Ref. 15)] has been recently proposed including tools for computation of dose deposit and absorbed energy for applications in both conventional radiotherapy and hadrontherapy. A feasibility study to assess these enhanced features dedicated to using GATE for conventional photon beam radiotherapy applications was performed recently.[15] This specific study demonstrated the feasibility of modeling a linear accelerator with GATE v6.0. Besides, an example for one patient was also given demonstrating the feasibility of a clinical evaluation using real treatments. Other studies exploring the new therapy related GATE capabilities have focused on the potential of this MC platform within the context of treatment planning dose calculation considering different proton beam configurations.[13,14]

On the other hand, several dosimetry accuracy studies comparing measurements and/or TPS results with different MC simulation based dose calculations for complex treatment techniques have been previously performed. In some of these studies, dose calculation algorithms were calibrated against dosimetry measurements using dedicated phantoms,[14–16] while other studies compared MC code dose calculation results with corresponding TPS dose calculations covering different clinical situations.[17–22]

The objective of this work is to further evaluate and validate the use of the GATE MC simulation platform for photon based radiotherapy treatment planning and associated clinical dosimetry studies. First, the comprehensive modeling of a clinical linear accelerator equipped with a state-of-the-art multileaf collimator (MLC) is performed and validated. As a second step, the GATE based simulation of IMRT treatment plans based on several head and neck cases was investigated and validated in terms of both relative and absolute dosimetry. To our knowledge, this is the first time that GATE has been evaluated in terms of absolute dosimetry calculations for multiple realistic clinical intensity modulated radiotherapy treatment plans.

II. MATERIALS AND METHODS

The GATE v6.1 simulation platform with the associated dose scoring tool was used to simulate the Siemens Oncor Impression™ (SIEMENS, Kemlat, Germany) linear accelerator. This platform allowed generating and monitoring different characteristics of interacting particles like position, energy, and direction. The modeling of the accelerator was validated by comparing dosimetry data derived from different beam simulations and corresponding measurements under realistic conditions. Several IMRT treatments were simulated and results were compared with real measurements using phantoms dedicated to clinical quality assurance.

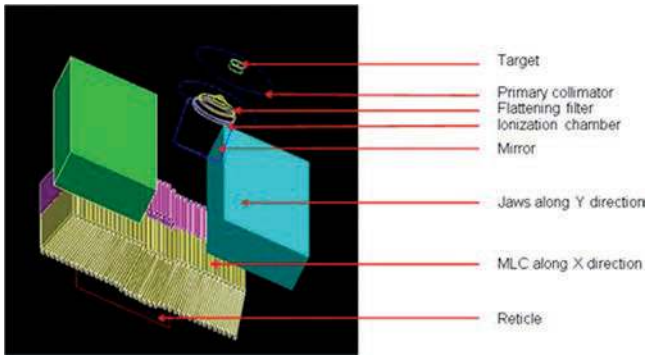

FIG. 1. The different components of the head of the accelerator as seen using the GATE interface display.

II.A. GATE physics settings for LINAC modeling

II.A.1. Geometry

The flexibility of GATE/Geant4 and the versatility of its macrointerface allow the modeling of physical and geometrical characteristics of the different components of the Siemens Oncor Impression accelerator. All these characteristics, in terms of shape, size, dimensions, and material, were defined according to the manufacturer specifications (Fig. 1). For this study, the modeling of the head of the LINAC is separated into two main modules (see Fig. 2):

(i) Module 1 or patient independent part: target, primary collimator, flattering filter, monitor chamber, and mirror.

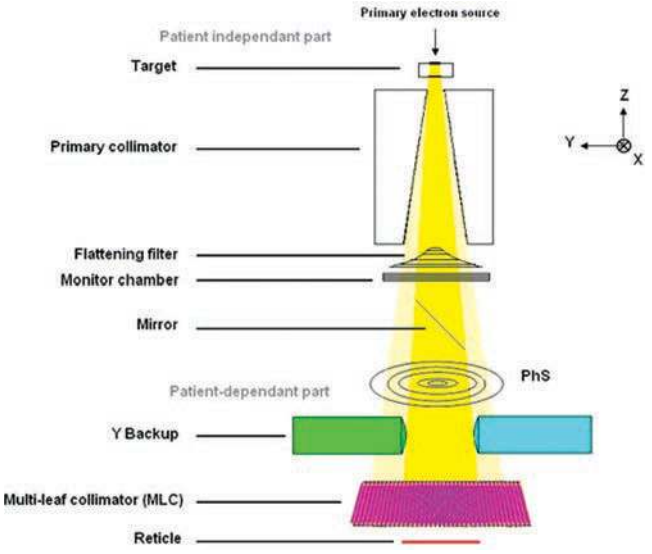

FIG. 2. Description of the different geometrical elements of the accelerator head of Siemens ONCOR, defining the two modules for simulation and the location of the PhS.

(ii) Module 2 or patient dependent part: additional collimator jaws Y, MLC, and reticle (see Fig. 2).

II.A.2. Electron source

The electron source is the most relevant element that determines the characteristics of the output beam. It is specified by two main features;[23] namely, the electron's mean energy and the spot size. A Gaussian distribution was assumed for the electron energy. An electron spot with full width at half maximum (FWHM) of 3 mm and a mean energy of 6.7 MeV with $\sigma = 0.077$ MeV was found to fit measurements.[15,24,25] These details were deduced from a photon characteristics study used to obtain a generalized source model for a 6 MV photon beam output, according to a comparison of energy distribution coordinates, radial distribution, depth doses and photon dose distribution between several source models. The mean energy determines both the percent depth dose (PDD) and the dose profiles shape (input dose, build-up region in depth, fluence distribution), while the spot size influences the shape and characteristics of dose profiles (width, dose in the center of the profile, gradient in the penumbra region).

II.A.3. Dose scoring tool

An energy/dose scoring associated with statistical uncertainty is used to calculate the energy deposition and absorbed dose in a matrix of dosels (dose voxels[26]).

This matrix is attached to the studied volume (water phantom, solid phantom, x-ray computed tomography of a given patient, and other measuring materials or devices).

Each time a particle registers a hit in the volume of interest, the amount of energy deposited in MeV and/or absorbed dose in Gy is stored in the corresponding dosel. Dosel sizes are set by the user and for this study a size of $5 \times 5 \times 5$ mm^3 was used, which corresponds to the 0.125 cm^3 sensitive volume of the ionization chamber used for measurement.

In GATE, the generated particles are collected in a particular virtual space called phase space (PhS). The PhS is more precisely developed to store the particles incoming from the patient independent part (module 1), and is committed to a volume of user-defined size, storing the characteristics of each particle (type, 3D coordinates, direction, energy, and final volume of interaction). In this simulation, the PhS is defined as a circular volume with a diameter of 20 cm and a thickness of 1 nm in the z direction, so all the particles stored in the PhS may be considered in the same z position (Fig. 3). The PhS is located at 7 cm above the second collimator (Y jaws, see Fig. 2).

II.A.4. Source model

The PhS file obtained is read directly to simulate the fluence of photons derived from the PhS made of three subsources called "multiple source model" (Ref. 27), and interacting with the patient-dependent part (module 2). Fluence of photons in the head of the accelerator results from interactions of primary electrons with the target, mainly by bremsstrahlung effect.[28] High-energy photons can scatter in this geometry, while those with lower energy are absorbed.

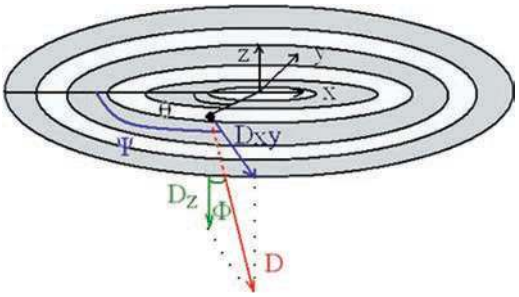

FIG. 3. Coordinate system in the phase space. Photon position is defined by the angle θ and the radial distance r. Photon direction is defined by the angles ψ and Φ. $\vec{D}$ is the photon direction of length D, composed of $\overrightarrow{D_{xy}}$: the azimuthal component in the xOy plan and $\overrightarrow{D_z}$: the vertical component. Φ is the angle between and in the vertical plan and ψ is the angle between and in the azimuthal plan.

Finally, the output beam consists of photons coming from the bremsstrahlung target directly, as well as secondary particles from the primary collimator, flattening filter, and the second collimator. Regarding the photon position and energy, the PhS was divided into 200 bins (rings) with a constant radial pitch of 0.5 mm. For each source (target, primary collimator, and flattening filter), a histogram of 200 bins containing the radial distribution of photons was synthesized. A histogram of the energy was associated to each ring, divided into 400 bins from 0 to 8 MeV with an energy step of 20 keV. Considering the direction of photons, the PhS was divided into 40 radial bins, with a pitch of 2.5 mm. An energy histogram of 20 bins was associated with each ring with a step of 400 keV. Two histograms for directions Φ and ψ were attributed for each energy bin of each ring. Such a double correlation in energy and radial position was found to reproduce precisely the photon fluence (Fig. 3).

PhS storing of between 2 and 170×10^6 photons have been proposed[24,25] depending mainly on the simulated field. In this study, 1×10^9 particles were stored in multiple PhS files which gave a total volume of 8.4 GB file stored as a ROOT file.[29]

II.B. Reference data for dose comparison

Experimental data consisted of a series of dose distribution measurements made either in water or in tissue equivalent phantoms. Measurements in water were performed using a tank filled with water and a motorized arm for an accurate ionization chamber positioning (MP3-M water phantom system, PTW, Freiburg, Germany). Two tissue-equivalent phantoms were used specifically for IMRT plan evaluation. The first phantom was a cylindrical RW3 phantom (matrix phantom model T40026, PTW) with 25 spaced holes allowing positioning an ionization chamber at different locations and depths. The second phantom was an octagonal phantom (Octavius model T40051, PTW) specifically designed for performing planar dose measurements. For this purpose, a planar ion chamber matrix (2D Array from PTW, 729 chambers in total) was inserted inside the phantom. The aim was first

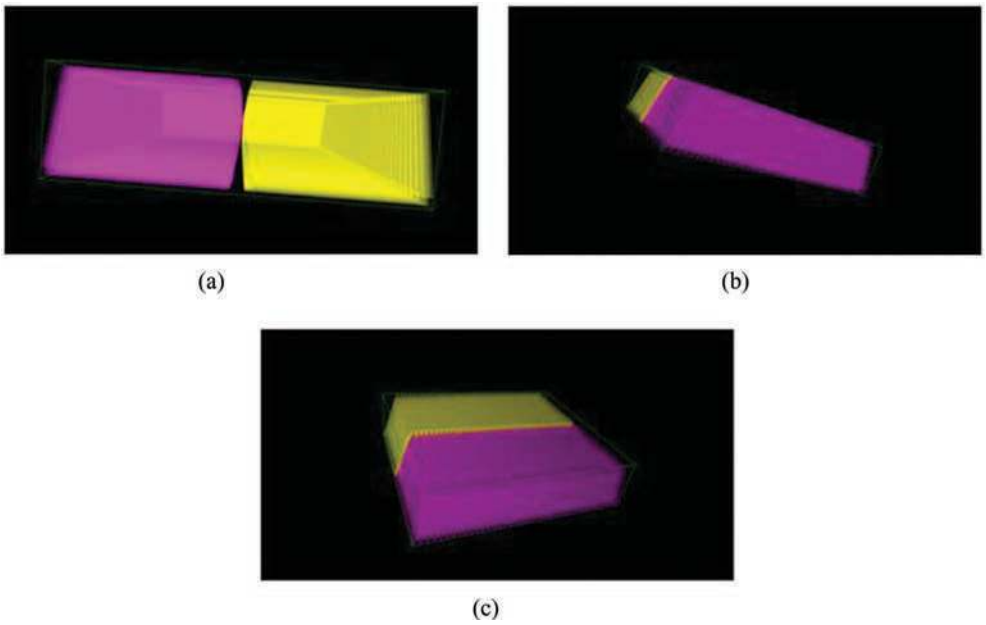

FIG. 4. Multileaf collimator device as modeled with GATE (a) leaf edges, (b) and (c) MLC X1 leaves bank (light color) and X2 leaves bank (dark color) seen from two points of view.

to obtain planar dose distributions for each IMRT beam, and as a second step to compare them with distributions coming from the same IMRT plans simulated with GATE. For this purpose, the same phantoms were also simulated with the GATE MC platform, while gamma-index computation was used for quantitative comparison of the corresponding dose distributions.

In order to evaluate the calculation of absolute dose per fraction for each beam, real measurements by an ionization chamber inside the cylindrical phantom were compared with the corresponding GATE calculations. Phantom data acquisition and analysis was monitored using dedicated software Verisoft 4.1 (PTW, Freiburg, Germany), allowing to compare two-dimensional (2D) dose matrices derived from measurements (2D-Array Matrix detector) and corresponding computed data using a radiotherapy treatment planning system.

II.C. Dosimetry study

The simulation results were compared with measurements made with a 160 MLC mounted on the Siemens Oncor linear accelerator. This state-of-the-art MLC consists of 160 leaves (two opposite banks of 80 leaves) with additional jaws in the transverse direction Y shaping a maximum radiation field of 400×400 mm^2. The leaves have a projected width of 5 mm in the Y direction for the entire field, and they are slightly titled in order to avoid a straight open air gap for central field's rays. Each bank of the MLC is arranged in an alternating pattern of upper and lower leaves. Both leaves types have the same height of 95 mm (Fig. 4), but the upper leaf is shifted slightly upwards compared to the lower leaf. Combined with the tilt of the leaves, this particular point leads to a different length of the overlap region between two neighboring leaves. For one pair of adjacent leaves, the top part of the upper leaf covers the bottom edge of a lower leaf resulting in a larger overlap than for the next adjacent leaf where the top edge of a lower leaf covers a shorter section of the bottom part of the upper leaf. This difference affects the interleaf leakage since it alternates the length of the overlap region.[30] It is important mentioning that manufacturer data concerning the leaf-end profile were incomplete and the exact curvature and dimensions of the slightly curved central part was not available. For this reason, it was chosen to approximate the leaf-end shape by a rounded shape, with a radius of 197.5 mm, a height of 5 mm, and an angle of 27.62°. The difference between actual and simulated shapes can be seen in Fig. 5. Leaf penumbra and leakage were studied specifically and compared to reference values.[30]

To validate the GATE LINAC model, a set of experimental measurements were performed in order to obtain typical dosimetric parameters:

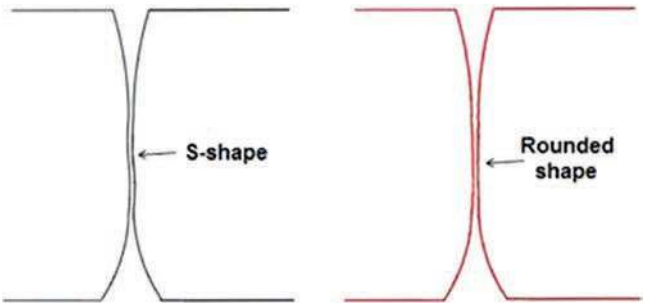

FIG. 5. Actual MLC leaf edge (left) and MLC leaf edge approximation as simulated with GATE. The small "S shape" at the center is not taken into account in the simulation because exact curvature and dimensions were not made available.

II.C.1. Tissue phantom ratio TPR_{10}^{20}

This parameter is defined as the ratio of the dose at 20 and 10 cm depth in water for a source to detector distance of 100 cm (IAEA TRS-398) and for a field size of 10 × 10 cm^2 at depth measurement. The TPR_{10}^{20} is the relevant parameter necessary to express the quality of high energy photon beams according to international recommendations.

II.C.2. PDD and transverse profiles

Percent depth doses were calculated with GATE in a water phantom, at depths ranging from 0 to 30 cm, for a 95 cm source to surface distance, with a resolution of 2 × 2 × 2 mm^3 and for different field sizes: 4 × 4, 5 × 5, 10 × 10, 15 × 15, 20 × 20, 25 × 25, 30 × 30, and 40 × 40 cm^2. Dose profiles across fields of identical sizes were calculated in the same conditions for a 95 cm source to surface distance and for a 15 mm depth in water.

II.C.3. Output factor

Measured and simulated output factors were the dose value at 5 cm depth in water for a source to surface distance of 95 cm for different square field sizes, normalized to the dose value for a square field of 10 × 10 cm^2.

II.D. Patient IMRT treatments

The particular aim of this part was to demonstrate the ability of GATE to perform reliable simulations of complex treatments comprising numerous small beams, which is typically the case in step-and-shoot IMRT. After validation of the LINAC model with the previously dosimetric study in water phantom, IMRT simulations were performed and validated according to the following procedure.

Seven head-and-neck IMRT treatment plans with different beam patterns were simulated using GATE as well as the modeled accelerator. The patients used in this study were actually treated with the modeled accelerator. Step-and-shoot IMRT treatments were planned using the Pinnacle™ v8.0 m treatment planning system (Philips Electronics, Netherlands). MLC positions for each segment of each beam were obtained by using direct machine parameters' optimization. They were subsequently exported from Pinnacle and adapted to allow GATE simulation.

II.D.1. Dose uncertainty

The dose uncertainty obtained for GATE simulations was evaluated according to several quantitative criteria. Statistical uncertainty in a dosel i was computed using the following equation:[23,31]

$$\sigma_i = \sqrt{\frac{1}{N-1}\left(\frac{\sum X_j^2}{N} - \left(\frac{\sum X_j}{N}\right)^2\right)}, \quad (1)$$

where, σ_i is an estimate of the standard error of the mean dose in the dosel i, N is the number of primary independent histories, and X_j the contribution to the scored quantity in the dosel. The simulation uncertainty was estimated using Equation (2):

$$\sigma_{D>0.5D_{\max}} = \sqrt{\frac{1}{K_{50}}\sum_{i=1}^{K_{50}}\left(\frac{\sigma_i}{D_i}\right)^2} \quad (2)$$

where K_{50} is the number of dosels that receive a dose higher than 50% of the maximal dose and $\left(\frac{\sigma_i}{D_i}\right)$ is the relative statistical uncertainty.

II.D.2. Experimental dose validation

The experimental model validation was done in two steps. First, through a comparison between modeled and measured relative planar doses using gamma index and second by comparing absolute doses at a given phantom location. This two-step approach in which relative and absolute doses are investigated separately is comparable with what is recommended for validation of clinical IMRT plans. For the relative comparison of planar doses, we used the Octavius Octagonal T40051 phantom for a source to point measurement distance of 99.6 cm. The 2D gamma index was calculated[32] between the GATE simulation and experimental measurements in a matrix detector inserted in the Octavius phantom and containing 729 detectors (27 × 27 detectors). For the calculation of 2D gamma index, the following constraints were imposed: 5% dose difference, 4.0 mm distance-to-agreement, discarding of doses below 10% of max dose in the measured dataset.

II.D.3. Absolute dose calibration

As a second validation step an absolute dose comparison was carried out using a different approach. First, a calibration of the simulated accelerator in terms of absolute dose per monitor unit was performed[33] using two distinct steps:

(i) Conventional calibration of the beam, by measuring the dose in water in Gy per Monitor Unit $D(A_{\text{ref}})$/MU at a 5 cm reference depth, for a source to surface distance of 100 cm in a reference field size of 10 × 10 cm^2 (A_{ref}). In our case, reference measurements were defined as 100 cGy for 100 MU at the reference depth.

(ii) GATE simulation of the same exact setup and associated conditions, using particles from the PhS file, in order to obtain $D_{\text{GATE}}(A_{\text{ref}})$ per simulated particle, which can be written as $D_{\text{GATE}/_{\text{part}}}(A_{\text{ref}})$.

A calibration factor F_Q for this particular beam was then derived

$$F_Q = \frac{D\,(A_{\text{ref}})\,/\text{MU}}{D_{\text{GATE}/_{\text{part}}}(A_{\text{ref}})}. \quad (3)$$

This factor depends on the beam quality (6 MV photons in our case[34]), and has the dimensions of particles per monitor unit.

After calibration and as a second stage of the absolute dose comparison process, beam simulation in water was replaced by IMRT simulation in the PTW Matrix Phantom T40026, the

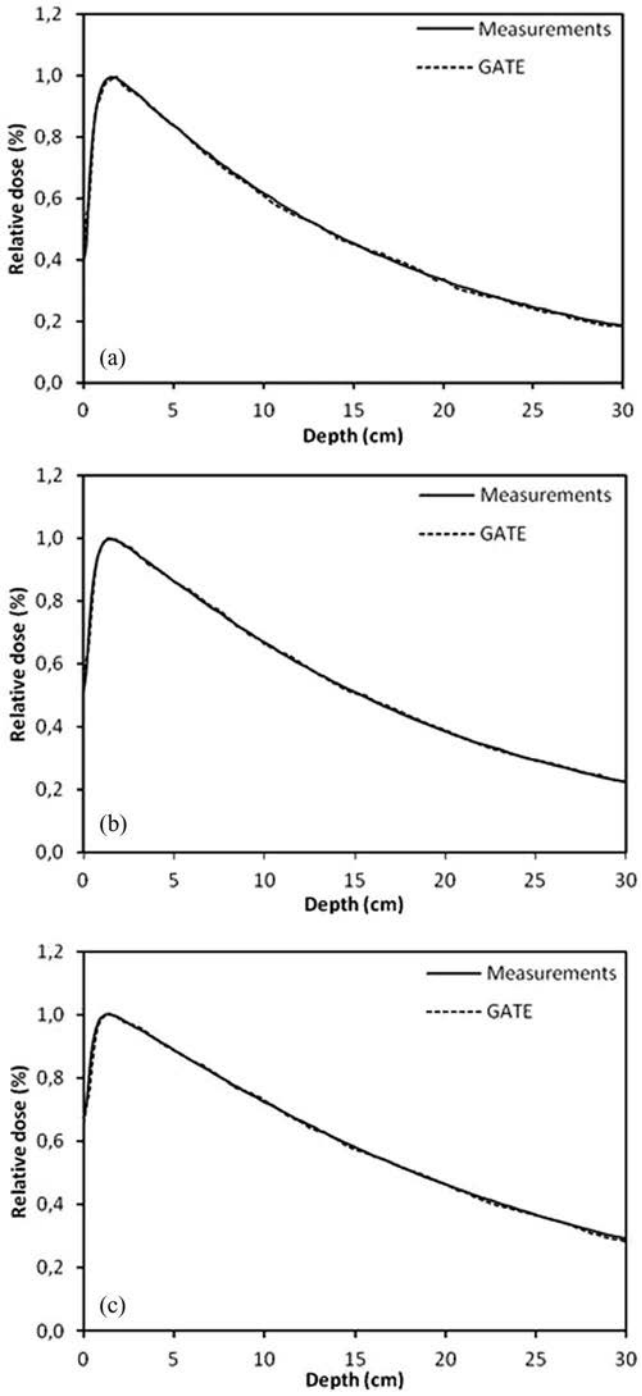

FIG. 6. Percent depth doses for three different field sizes (a) 4 × 4, (b) 10 × 10 and (c) 40 × 40 cm^2.

field size being adjusted to each beam of the IMRT treatment plan, A_{beam}. More precisely, a new GATE simulation was done for each beam of each IMRT from the PhS file (5×10^8 particles for each beam), yielding a dose $D_C(A_{\text{beam}})\text{GATE}/_{\text{part}}$, at the point C inside the phantom. This point was chosen as the phantom center, positioned at the isocenter of the accelerator. The absolute dose in Gy per monitor unit at C is given by

$$\frac{D_C\,(A_{\text{beam}})}{\text{MU}} = F_Q \times D_C\,(A_{\text{beam}})\,\text{GATE}/_{\text{part}}. \qquad (4)$$

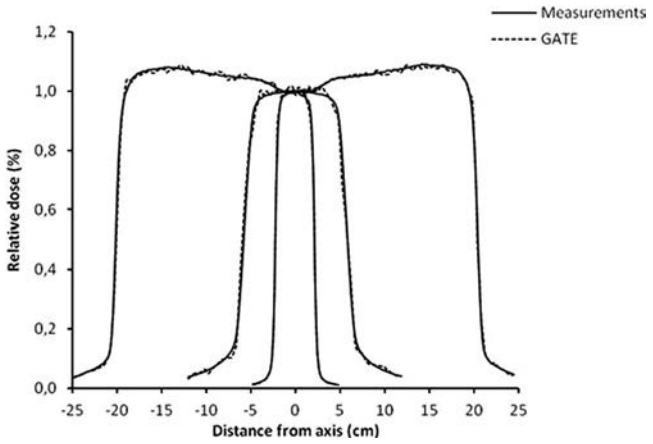

FIG. 7. Transverse profiles for fields 4 × 4, 10 × 10 and 40 × 40 cm^2 obtained with both simulation and measurements (across X direction).

As a consequence the absolute dose at C for each beam, in Gy, is

$$D_C\,(A_{\text{beam}}) = \text{MU} \times F_Q \times D_C\,(A_{\text{beam}})\,\text{GATE}/_{\text{part}} \qquad (5)$$

with MU the number of monitor units calculated by the TPS.

III. RESULTS

III.A. Dosimetry measurements

The tissue phantom ratio TPR_{10}^{20}, obtained for the 6 MV photon beam after GATE simulation was 0.672 ± 0.063, and within 0.44% compared to the value measured experimentally (0.675) using the same setup as that simulated. Simulated percent depth doses and corresponding errors relative to measurements were calculated between 0 and 30 cm. As an illustration three examples are given in Fig. 6, for 4 × 4, 10 × 10, and 40 × 40 cm^2 field sizes. Transverse dose profiles for comparable fields are shown in Fig. 7. Statistical uncertainties and errors with measurements are given in Tables I and II for a wide range of field sizes. Dose profiles were determined from a large transverse line compared to the

TABLE I. Percent depth dose: GATE statistical uncertainties and errors relative to measurements.

	GATE uncertainty (%)		Error (%)	
	Mean	Standard deviation	Mean	Standard deviation
Field 4 × 4 cm^2	0.104	0.046	1.703	1.636
Field 5 × 5 cm^2	0.104	0.053	1.487	1.018
Field 10 × 10 cm^2	0.048	0.009	0.942	0.697
Field 15 × 15 cm^2	0.113	0.052	1.686	1.241
Field 20 × 20 cm^2	0.112	0.063	1.777	1.469
Field 25 × 25 cm^2	0.123	0.057	1.331	1.203
Field 30 × 30 cm^2	0.134	0.064	1.615	1.306
Field 40 × 40 cm^2	0.105	0.050	1.238	1.082
Mean	0.105	0.049	1.472	1.207
Standard deviation	0.025	0.017	0.285	0.287

TABLE II. Dose profiles: GATE statistical uncertainties and errors relative to measurements.

	GATE uncertainty (%)		Error (%)	
	Mean	Standard deviation	Mean	Standard deviation
Field 4 × 4 cm^2	0.232	0.146	3.727	3.4
Field 5 × 5 cm^2	0.331	0.195	5.829	4.923
Field 10 × 10 cm^2	0.221	0.093	6.288	6.094
Field 15 × 15 cm^2	0.182	0.138	6.482	8.914
Field 20 × 20 cm^2	0.167	0.122	5.374	7.82
Field 25 × 25 cm^2	0.183	0.132	3.745	5.462
Field 30 × 30 cm^2	0.177	0.124	4.143	5.894
Field 40 × 40 cm^2	0.155	0.074	3.03	4.459
Mean	0.206	0.128	4.827	5.871
Standard deviation	0.057	0.036	1.323	1.784

radiation field size, which probably tends to lower the mean error for fields 4 × 4 and 5 × 5 cm^2. Globally, the small differences between measurements and simulated results suggest that the various accelerator components were accurately modeled.

Established for square fields, the output factor describes the relative variation of the dose output with increasing size of fields (Fig. 8). The maximum error obtained was of 1.22% for the 3 × 3 cm^2 field (small field), while for all fields considered errors were 0.497% ± 0.397%. This low level of discrepancy on the output factor suggests that the simulated dose rate is close to the actual dose rate.

Results concerning the modeling of the MLC are now presented. The leaf-end penumbra was obtained by calculating the dose profile below one leaf bank closed and the other bank open [Fig. 9(a)]. The penumbra was measured between 20% and 80% of the dose maximum and the obtained value was 6.2 ± 0.8 mm which is in agreement with the manufacturer specifications (less than 7 mm), even if the profile shape was partially simplified in the present modeling (Fig. 5).

The leaf-side penumbra [Fig. 9(b)] was defined as the distance between 20% and 80% of dose maximum from a

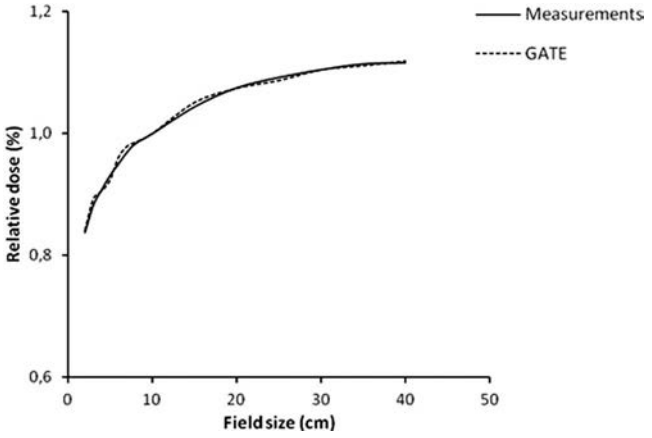

FIG. 8. Output factor curve obtained with different sizes of open fields. Maximum error was 1.22% for a field size 3 × 3 cm^2.

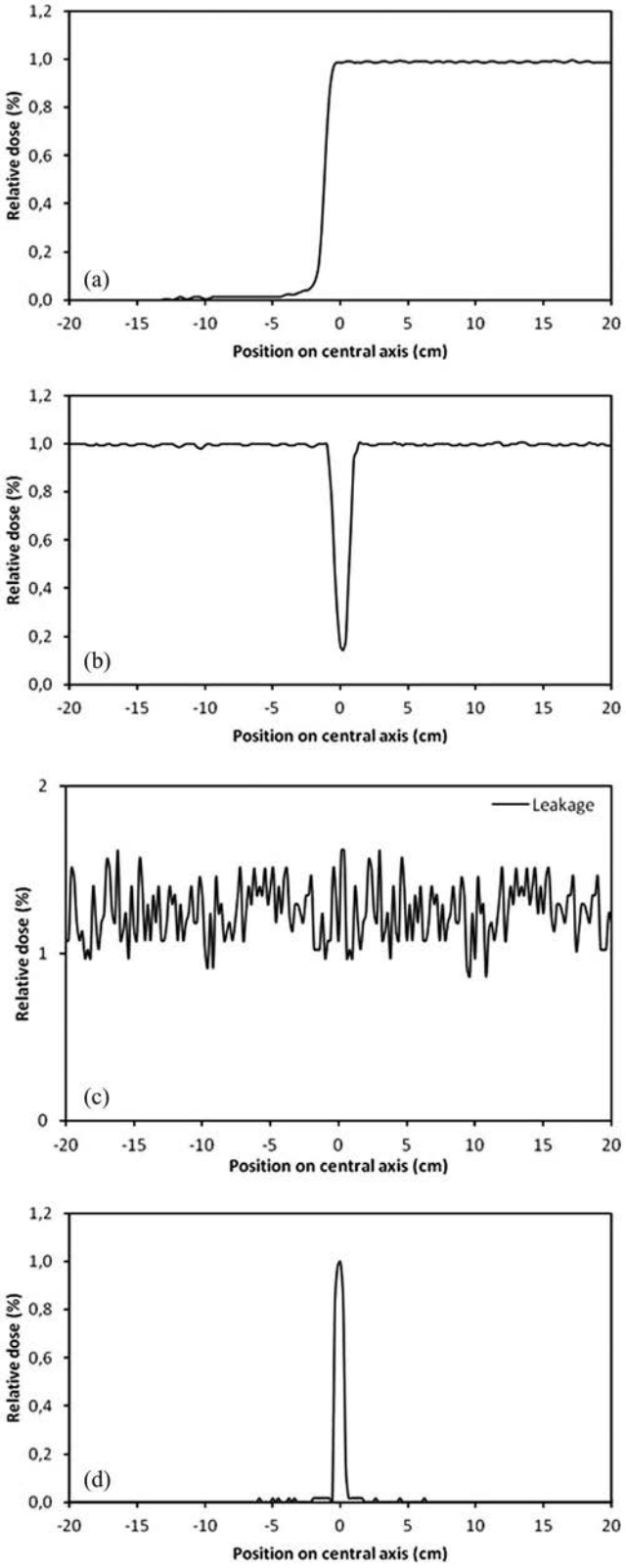

FIG. 9. (a) Transverse profile obtained below one MLC bank closed (Y jaws fully retracted at position +20 and −20 cm). (b) Transverse profile obtained in the Y direction, below MLC banks fully retracted, excepted one leaf positioned at 0 cm. (c) Interleaf leakage obtained as the transverse profile in the Y direction below MLC banks completely closed, while Y jaws stay fully retracted (positioned at ±20 cm). (d) Leaf gap obtained in the transverse profile below MLC banks closed at 15 mm depth in water. The FWHM was 9.0 ± 0.5 mm.

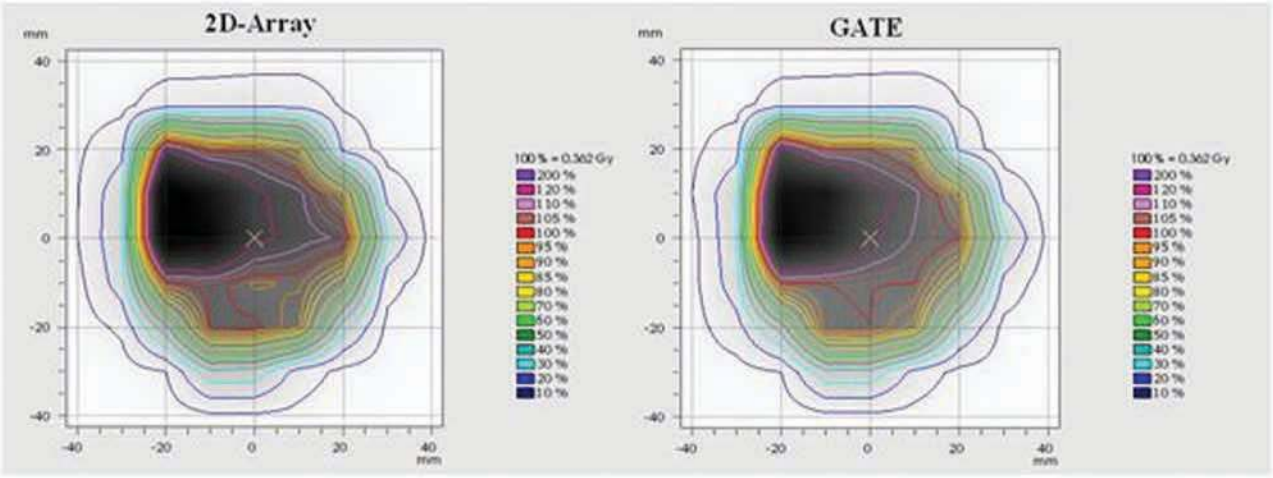

FIG. 10. Isodose maps obtained with the PTW Verisoft software for GATE (right) and 2D-array measurements (left) for patient 6, beam 0.

transverse profile in the Y axis, with both leaf banks fully retracted, excepted one leaf positioned at 0 mm. The penumbra calculated in +Y direction was 5.4 ± 0.5 mm, and 6.5 ± 0.3 mm in the −Y direction, which is similar to previously published data concerning dosimetric evaluation of this MLC.[30] The interleaf leakage was calculated as the dose profile below closed MLC banks [Fig. 9(c)], with both Y1 and Y2 jaws fully retracted. The interleaf leakage obtained by simulation was 1.25% ± 0.17% while the experimental value was 0.76% across the entire field. Published values[30] ranged from 0.4% to 1.2% depending on the measurements method and experimental setup. Leaf gap was evaluated using a dose profile in the X direction, with the two leaf banks kept closed (in this configuration, opposite leaves were in contact). The FWHM obtained from the profile [Fig. 9(d)] was 9.0 mm ± 0.5 mm, which is comparable to previously published data.[30]

III.B. IMRT treatment planning

As described previously in Sec. II.D, seven head-and-neck patient IMRT plans (Table III) were simulated in order to clearly demonstrate the ability of the GATE platform to simulate clinical radiotherapy treatments, especially when one considers complex field shape configurations obtained using the MLC. The simulated IMRT treatment plans were compared to experimental measurements using phantoms dedicated to quality assurance of IMRT treatments. Quantitative criteria were used based on standard international recommendations for validation of clinical beams.

TABLE III. Configuration of the simulated IMRT treatment plans (beam orientation in deg). Patient 1 had a two phase treatment and phase B was a boost.

Patient	Treatment phase	Configuration of the beams (gantry angles in deg)
Patient 1	A	0°, 50°, 100°, 230°, 260° and 310°
	B	0°, 50°, 100°, 230°, 260° and 310°
Patient 2	A	0°, 50°, 100°, 210°, 260° and 310°
Patient 3	A	0°, 50°, 100°, 260° and 310°
Patient 4	A	0°, 40°, 80°, 120° and 150°
Patient 5	A	0°, 50°, 100°, 230°, 260° and 310°
Patient 6	A	0°, 35°, 70°, 105° and 140°

Relative comparison was done by means of planar dose gamma-index computation for each beam, as seen in Fig. 10 where the 2D dose distribution, simulated in the Octavius phantom for patient 6 with the 0° beam (5 segments), is shown. In this case, among the 30 evaluated points, 29 points (96.7%) passed the 5%/4 mm test (for validation of clinical beams, international recommendations suggest that at least 85% of the points pass the 5%/4 mm test).[35] For this same beam, the mean gamma value was 0.295 and the relative statistical uncertainty was 0.091%. Corresponding isodose maps for both GATE simulation and experimental measurements are given in Fig. 11. Gamma index for all seven patients are reported in Table IV, while the percentage of the dose points satisfying the 5% in dose and 4 mm in distance-to-agreement criteria are reported in Table V.

Before performing absolute dose simulations, a calibration step of the accelerator in the GATE platform was mandatory (see Sec. II.B). The parameters obtained for this purpose were

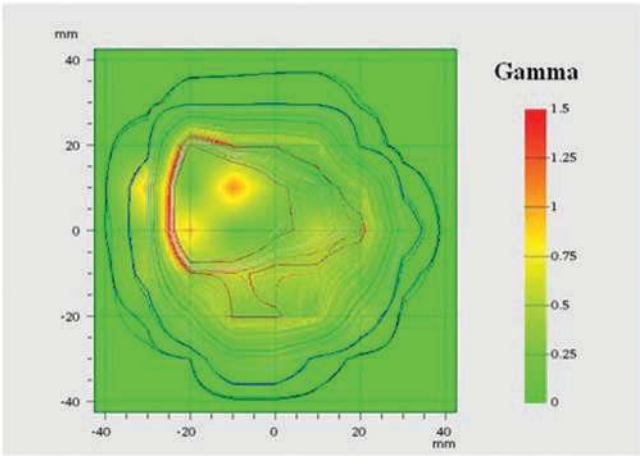

FIG. 11. Gamma distribution obtained for the Gamma-index calculation of the beam 0° for the patient 6.

TABLE IV. 2D gamma-index evaluation between experimental measurements with a planar detector and simulation with GATE (gamma values).

Patient	Mean gamma value	Median gamma value	Maximum gamma value
Patient 1 A	0.570	0.727	0.839
Patient 1 B	0.624	0.623	0.724
Patient 2	0.633	0.628	0.788
Patient 3	0.334	0.277	0.534
Patient 4	0.513	0.509	0.769
Patient 5	0.409	0.396	0.541
Patient 6	0.297	0.298	0.345

$D_{GATE}(A_{ref}) = 1.05 \times 10^{-7}$Gy for 2×10^9 particles from the PhS in reference conditions, and $F_Q = 1.90 \times 10^{+14}$ particles per monitor unit. For each patient, the dose per fraction (in Gy) for each beam measured with an ionization chamber at the center of the specific phantom and obtained with the corresponding GATE calculations at the same phantom location are reported in Table VI. The uncertainties for absolute dose calculations in the volume of interest using GATE, including mean and standard deviation for the seven plans are reported in Table VII.

Apart from this global analysis, more detailed results are also provided for patient 6 as an example (Tables VIII–X).

TABLE V. Simulated and experimental planar dose comparison for IMRT plans: Number of dose points passing the gamma-index test.

Patient	Treatment angle (deg)	Percentage of dose points passing the 5%/4 mm criterion	Total number of dose points	GATE statistical uncertainty (%)
Patient 1A	A0	84.2	38	0.268
	A50	81.1	53	0.204
	A100	93.3	59	0.182
	A230	87.5	56	0.176
	A260	90.2	61	0.203
	A310	91.8	49	0.211
Patient 1B	B0	100	23	0.195
	B50	100	32	0.185
	B100	100	26	0.174
	B230	87.9	33	0.206
	B260	100	32	0.184
	B310	100	30	0.205
Patient 2	A0	84.4	301	0.194
	A50	83.5	297	0.196
	A100	81.0	247	0.188
	A150	86.9	289	0.195
	A210	92.6	283	0.187
	A260	89.5	239	0.201
	A310	94.9	297	0.183
Patient 3	A0	83.7	43	0.099
	A50	85.3	34	0.101
	A100	90.5	42	0.115
	A260	94.4	36	0.105
	A310	88.1	42	0.100
Patient 4	A0	87.7	146	0.107
	A40	87.7	220	0.121
	A80	90.9	220	0.135
	A120	86.7	190	0.113
	A150	96.0	151	0.116
Patient 5	A0	92.3	246	0.285
	A50	86.3	227	0.223
	A100	91.0	189	0.185
	A150	89.7	195	0.211
	A210	92.6	190	0.292
	A260	96.7	182	0.187
	A310	93.9	196	0.17
Patient 6	A0	96.7	30	0.091
	A35	100	31	0.098
	A70	93.8	32	0.143
	A105	100	31	0.095
	A140	100	29	0.143

TABLE VI. Monitor unit calibration and absolute dose calculation (at the isocenter).

Patient	Absolute dose according to GATE (Gy/fraction)	Absolute dose according to measurements (Gy/fraction)	Difference (%)
Patient 1 A	1.596	1.590	0.377
Patient 1 B	1.634	1.622	0.740
Patient 2	1.756	1.751	0.286
Patient 3	1.713	1.718	0.320
Patient 4	1.630	1.643	0.779
Patient 5	1.688	1.695	0.413
Patient 6	2.006	2.008	0.099

In Tables VIII–X, respectively, one can see, for each beam, the number of points within the 5%/4 mm criterion, mean, medium, and maximum gamma values, and both measured and simulated absolute doses. It is worth noticing that the difference between simulated and measured dose for the whole fraction was less than 1%.

In terms of calculation time, the simulation for each IMRT plan/phase, considering 5×10^8 simulated photons per beam, was 12 h in a cluster of 100 CPUs (2.74 GHz, 2 GB memory/CPU).

IV. DISCUSSION

The first objective of this study was to use the GATE platform to model a linear accelerator with a state-of-the-art multileaf collimator and to validate the obtained modeling by comparison with experimental measurements. The second objective was to use the modeled system to simulate clinical applications in radiotherapy through a series of step-and-shoot IMRT treatment plans. Here again, the validation step involved a comparison with experimental measurements using physical phantoms dedicated to quality assurance.

In order to ensure a sufficient accuracy, it was necessary to correctly model the different parts constituting the head of the accelerator and in particular the 160 MLC and its complex structure (in the limit of manufacturer data availability). This step was greatly facilitated by the GATE interface based on user-friendly macrofunctions and easy-to-use graphical environment. Accurate physical settings were made possible by the development of advanced energy/dose scoring tools and the definition of a specific phase space.

The quantitative validation of the developed simulated model was performed by extracting several typical dosimetry parameters from standard beam simulations, made in reference conditions, and by comparing them with measurements obtained in the exact same reference conditions. More specifically, the tissue phantom ratio results obtained with the simulation platform confirms that the simulated high energy 6 MV photon beam has similar quality in terms of particle fluence as the actual beam produced by the simulated accelerator (0.44% error). In addition, the simulated depth dose and transverse profile results were $<1.472\% \pm 0.285\%$ and $<4.827\% \pm 1.323\%$, of the corresponding measured depth dose and profiles, respectively. For dose profiles, the higher level of error may be explained by the presence of high dose gradient in the penumbra leading to higher relative errors between simulated and experimental curves. Another reason could be the approximation concerning the leaf-end shape modeling compared with actual shape (see Fig. 5). These results, however, suggest that no significant errors or biases were introduced by the simulated model and that the different accelerator components were modeled with very suitable accuracy. These model validation results suggest that the developed simulation model is sufficiently precise, thus, providing the potential for a high accuracy in the patient IMRT simulations.

Results from the IMRT patient dosimetry studies demonstrate the ability and associated accuracy of GATE for realistically simulating complex clinical radiotherapy treatment plans. The calculation of the 2D gamma index provides a quantitative assessment of the quality of the Monte Carlo simulated with respect to the corresponding real measurements in a dedicated phantom. This point is also in accordance with a

TABLE VII. GATE absolute dose uncertainties (mean and standard deviation).

Patient	Treatment phase	GATE absolute dose uncertainty (%)	
		Mean	Standard deviation
Patient 1	A	0.135	0.007
	B	0.156	0.033
Patient 2	A	0.120	0.019
Patient 3	A	0.099	0.034
Patient 4	A	0.128	0.006
Patient 5	A	0.146	0.053
Patient 6	A	0.104	0.019

TABLE VIII. Results for relative dose comparison (patient 6).

Beam	Number of evaluated points	Number of points passing the test (5%/4 mm)
Beam 0°	30	29 (96.7%)
Beam 35°	31	31 (100%)
Beam 70°	32	30 (93.8%)
Beam 105°	31	31 (100%)
Beam 140°	29	29 (100%)

TABLE IX. Results for 2D gamma index (patient 6).

2D gamma index		
Mean	Median	Max
0.345	0.189	0.804
0.227	0.211	0.768
0.298	0.255	0.672
0.343	0.254	0.726
0.271	0.188	1.115

TABLE X. Results for absolute dose comparison (patient 6).

Phase A	GATE absolute dose (Gy/fraction)	Measurement absolute dose (Gy/fraction)	Difference (%)
Beam 0°	0.883	0.889	0.686
Beam 35°	0.173	0.174	0.747
Beam 70°	0.177	0.176	0.568
Beam 105°	0.130	0.129	0.853
Beam 140°	0.643	0.640	0.453
Total dose/fraction	2.006	2.008	0.099

comparative qualitative assessment of the obtained simulated and measured isodose maps.

All absolute dose simulated calculations were made possible using a simple cross-calibration approach that can be applied to any linear accelerator modeling. Simulated delivery of monitor units according to IMRT plans defined by the Pinnacle TPS gave concordant results with actual measurements obtained from IMRT quality assurance measurements, as performed in routine clinical radiotherapy treatment with a dedicated experimental setup (cylindrical matrix phantom and ionization chamber). Recommendations about tolerance level for acceptance of IMRT plans in terms of absolute dose generally indicate 5% per fraction.[36] Results obtained in the present study are consistent with this limit since the global error was $0.431\% \pm 0.246\%$.

Considering relative dose comparison studies, a treatment plan based on CT images of a homogeneous phantom has been previously used[13] to validate GATE relative to XiO TPS (Elekta, Sweden) against measurements. In this study, comparing GATE and XiO TPS results with measurements, more than 96% of the points passed a 3%/3 mm gamma evaluation. Within the same context of relative dose comparisons in our study concentrating on clinical IMRT treatment plans, 90.8% of the points considering all plans for seven different patient datasets passed the test 5%/4 mm. Part of this reduced accuracy could be attributed to the difference between actual and simulated shapes of MLC leaf end. However, there are significant differences also between the two studies concerning particles, beams, and size of radiation fields. For this reason, results remain difficult to compare directly. Another factor could be the larger patient variability considering that seven different IMRT plans were used in the present study. These results need to be confirmed on a larger patient database.

Concerning the absolute dose calculations, our results show a difference of less than 1% between the GATE simulated results and corresponding measurements for the selected clinical IMRT plans. This performance is better or at least comparable to that observed for other MC codes. More specifically on the use of MC simulation codes within an absolute dose calculation context, a percentage difference of $<2\%$ was found for a dynamic 7-field IMRT plan implemented in BEAMnrc/DOSXYZnrc (Ref. 21) using CT datasets of a cylindrical phantom. In addition, within a clinical comparison framework, using the enhanced collapsed cone algorithm versus the XVMC MC simulation code gave mean dose prediction errors of $<3\%$ for the planning target volume in 8 IMRT and 2 stereotactic body radiotherapy lung cases.[18]

Even if quantitative results obtained in the present study are in accordance with tolerance levels for clinical treatments, it may be of interest to determine the best accuracy achievable with GATE simulations. This objective was not within the framework of this study and would require a specific experimental setup including film dosimetry for higher spatial resolution results. In the same way, performance comparison with treatment planning systems, regarding management of tissue heterogeneities for example, could be relevant for both standard and IMRT plans and could be considered in future studies.

V. CONCLUSIONS

In this work, we have successfully used the GATE/Geant4 Monte Carlo simulation platform with the new module dedicated to radiation therapy to evaluate dose distributions associated with a comprehensively simulated clinical linear accelerator. The dose scoring tool and the PhS, which allows storing a large number of particles allow to perform radiotherapy simulations with results close to measurements performed under realistic conditions. The accuracy of the calculations obtained with GATE (gamma index, relative and absolute dose) has permitted to validate not only the accelerator simulated model based on phantom studies but also complete patient IMRT treatment plans. The accuracy assessment of the simulated IMRT treatment plans was based on methodology and associated acceptance criteria in agreement with international recommendations. As a future study, research should consider the integration of dynamic aspects either from the patient point of view (physiological movements as described by 4D anatomico-functional imaging, for example) or from the accelerator point of view (dynamic arc-therapy). Image-guided radiotherapy and dose-guided radiotherapy are also domains of interest that could be investigated with the GATE simulation platform.

ACKNOWLEDGMENT

This work was funded by a grant from the French research ministry.

[a] Author to whom correspondence should be addressed. Electronic mail: Saadia@Benhalouche@etudiant.univ-brest.fr

[1] L. Wang, C.-S. Chui, and M. Lovelock, "A patient-specific Monte Carlo dose-calculation method for photo beams," Med. Phys. **25**, 867–878 (1998).

[2] M. Fragose, N. Wen, S. Kumar, D. Liu, S. Ryu, B. Movsas, A. Munther, and I. J. Chetty, "Dosimetric verification and clinical evaluation of a new commercially available Monte Carlo based dose algorithm for application in stereotactic body radiation therapy (SBRT) treatment planning," Phys. Med. Biol. **55**, 4445–4454 (2010).

[3] L. Brualla, R. Palanco-Zamor, K. P. Steuhl, N. Bornfeld, and W. Sauerwein, "Monte Carlo simulations applied to conjunctival lymphoma radiotherapy treatment," Strahlenther. Onkol. **187**, 492–498 (2011).

[4] N. Chofor, D. Harder, K. Willborn, A. Rühmann, and B. Poppe, "Low-energy photons in high-energy photon fields-Monte Carlo generated spectra and a new descriptive parameter," Z. Med. Phys. **21**, 183–197 (2011).

[5]J. Sempau, A. Badal, and L. Brualla, "A PENELOPE-based system for the automated Monte Carlo simulation of clinacs and voxelized geometries application to far-from-axis fields," Med. Phys. **38**, 5887–5895 (2011).
[6]J. Belec, N. Ploquin, D. J. L. Russa, and B. G. Clark, "Position-probability-samplet Monte Carlo calculation of VMAT, 3DCRT, step-shoot IMRT and helical tomotherapy dose distributions using BEAmnrc/DOSXYZnrc," Med. Phys. **38**, 948–964 (2011).
[7]M. Fippel, "Fast Monte Carlo dose calculation for photon beams based on the VMC electron algorithm," Med. Phys. **26**, 1466–1475 (1999).
[8]C. R. Schmidtlein, A. S. Kirov, S. A. Nehmeh, Y. E. Erdi, J. L. Humm, H. I. Amols, L. M. Bidaut, A. Ganin, C. W. Stearns, D. L. McDaniel, and K. A. Hamacher, "Validation of GATE Monte Carlo simulations of the GE Advance/Discovery LS PET scanners," Med. Phys. **33**, 198–208 (2006).
[9]J. De Beenhouwer, S. Steve, V. Stefaan, V. Jeroen, V. H. Roel, R. Erwann, and L. Ignace, "Physics process level discrimination of detections for GATE: Assessment of contamination in SPECT and spurious activity in PET," Med. Phys. **36**, 1053–1060 (2009).
[10]C. O. Thiam, V. Breton, D. Donnarieix, B. Habib, and L. Maigne, "Validation of a dose deposited by low-energy photons using GATE/GEANT4," Phys. Med. Biol. **53**, 3039–3055 (2008).
[11]K. Assié, I. Gardin, and I. Buvat, "Validation of the Monte Carlo simulator GATE for indium-111 imaging," Phys. Med. Biol. **50**, 3113–3126 (2005).
[12]R. Taschereau, P. L Chow, and A. F. Chatziioanno, "Monte Carlo simulations of dose from microCT imaging procedures in a realistic mouse phantom," Med. Phys. **33**, 216–224 (2006).
[13]L. Grevillot, D. Bertrand, F. Dessy, N. Freud, and D. Sarrut, "GATE as a GEANT4-based Monte Carlo platform for the evaluation of proton pencil beam scanning treatment plans," Phys. Med. Biol. **57**, 4223–4244 (2012).
[14]J. Ströbele, T. Shreiner, H. Fuchs, and D. Georg, "Comparison of basic features of proton and helium ion pencil beams in water using GATE," Z. Med. Phys. **22**, 170–178 (2011).
[15]L. Grevillot, T. Frisson, N. Zahra, J.-N. Badel, and D. Sarrut, "Simulation of a 6 MV Elekta Precise Linac photon beam using GATE/GEANT4," Phys. Med. Biol. **56**, 903–918 (2011).
[16]P. Carrasco, N. Jornet, M. A. Duch, and L. Weber, "Comparison of dose calculation algorithms in slab phantoms with cortical bone equivalent heterogeneities," Med. Phys. **34**, 3323–3333 (2007).
[17]I. Fotina, P. Winler, T. ¨Künzler, J. Reiterer, I. Simmat, and D. Georg, "Advanced kernel methods vs. Monte Carlo-based dose calculation for high energy photon beams," Radiother. Oncol. **93**, 645–653 (2009).
[18]I. Fotina, G. Kragl, B. Kroupa, R. Trausmuth, and D. Georg, "Clinical comparison of the dose calculation using the enhanced collapsed cone algorithm vs. a new Monte Carlo algorithm," Strahlenther. Onkol. **187**, 433–441 (2011).
[19]L. Bogner, J. Scherer, M. Treutwein, M. Hartmann, F. Gum, and A. Amediek, "Verification of IMRT: Techniques and problems," Strahlenther. Onkol. **180**, 340–350 (2004).
[20]O. Koelbl, T. Krieger, U. Haedinger, O. Suer, and M. Flent, "Influence of calculation algorithm on dose distribution in irradiation of non-small cell lung cancer (NSCLC) collapsed cone versus pencil beam," Strahlenther. Onkol. **180**, 783–788 (2004).
[21]I. A. Popescu, C. P. Shaw, S. F. Zavgorodni, and W. A. Beckham, "Absolute dose calculations for Monte Carlo simulations of radiotherapy," Phys. Med. Biol. **50**, 3375–3392 (2005).
[22]B. Vanderstraeten, N. Reynaert, I. Madani, L. Paelinck, C. D. Wagter, W. d. Gersem, W. D. Neve, and H. Thierens, "Accuracy of patient dose calculation for lung IMRT: A comparison of Monte Carlo, convolution/superposition, and pencil beam computations," Med. Phys. **33**, 3149–3158 (2006).
[23]I. Chetty, B. Curran, J. E. Cygler, J. J. DeMarco, G. Ezzell, B. A. Faddegon, I. Kawrakow, P. J. Keall, H. Liu, C. M. Ma, D. W. Rogers, J. Seuntjens, D. Sheikh-Bagheri, and J. V. Siebers, "Report of the AAPM Task Group No. 105: Issues associated with clinical implementation of Monte Carlo-based photon and electron external beam treatment planning," Med. Phys. **34**, 4818–4853 (2007).
[24]M. K. Fix, P. J. Keall, K. Dawson, and J. V. Siebers, "Monte Carlo source model for photon beam radiotherapy: Photon source characteristics," Med. Phys. **31**, 3106–3121 (2004).
[25]M. K. Fix, P. J. Keall, and J. V. Siebers, "Photon-beam subsource sensitivity to the initial electron-beam parameters," Med. Phys. **32**, 1164–1175 (2005).
[26]D. Sarrut and L. Guigues, "Region-oriented CT image representation for reducing computing time of Monte Carlo simulations," Med. Phys. **35**, 1452–1463 (2008).
[27]M. K. Fix, P. Manser, E. J. Born, R. Mini, and P. Rüegsegger, "Monte Carlo simulation of a dynamic MLC based on a multiple source model," Phys. Med. Biol. **46**, 3241–3258 (2001).
[28]M. Krmar, D. Nikolic, P. Krsdtonosic, S. Cora, P. Francescon, P. Chiovati, and A. Rudic, "A simple method for bremsstrahlung spectra reconstruction form transmission measurement," Med. Phys **29**, 932–939 (2002).
[29]F. Rademakers and R. Brun, "ROOT: An object oriented data analysis framework," Linux J. (1998).
[30]M. B. Tacke, S. Nill, P. Häring, and U. Oelke, "6 MV dosimetric characterization of the 160 MLC, the new Siemens multileaf collimator," Med. Phys. **35**, 1934–1942 (2008).
[31]I. J. Chetty, M. Rosu, M. L. Kessler, B. A. Fraass, R. K. T. Haken, F. M. Kong, and D. L. McShan, "Reporting and analyzing statistical uncertainties in Monte Carlo-based treatment planning," Int. J. Radiat. Oncol., Biol., Phys. **65**, 1249–1259 (2006).
[32]D. A. Low, W. B. Harms, S. Mutic, and J. A. Purdy, "A technique for the quantitative evaluation of dose distributions," Med. Phys. **25**, 656–661 (1998).
[33]A. Nahum, "Special features of Monte Carlo based treatment planning," *The Handbook of Radiotherapy Physics: Theory and Practice* (Taylor & Francis, New York, 2007), Chap. 28, pp. 615–617.
[34]M. Pasler, D. Georg, H. Wirtz, and J. Lutterbach, "Effect of photon-beam energy on VMAT and IMRT treatment plan quality and dosimetric accuracy for advanced prostate cancer," Strahlenther. Onkol. **187**, 792–798 (2011).
[35]International Commission in Radiation Units and Measurements, "Prescribing, recording and reporting photon-beam intensity-modulated radiation therapy (IMRT)," ICRU Report No. 83 (ICRU Publications, 2010).
[36]S. Zefkili, M. Tomsej, P. Aletti, F. Bidault, A. Bridier, V. Marchesi, and S. Marcié, "Recommendations for a head and neck IMRT quality assurance protocol," Cancer Radiother. **8**, 364–379 (2004).